Disruption of the ESX-5 system of *Mycobacterium tuberculosis* causes loss of PPE protein secretion, reduction of cell wall integrity and strong attenuation

**Daria Bottai,[1]* Mariagrazia Di Luca,[1]
Laleh Majlessi,[2,3] Wafa Frigui,[4] Roxane Simeone,[4]
Fadel Sayes,[2,3] Wilbert Bitter,[5] Michael J. Brennan,[6]
Claude Leclerc,[2,3] Giovanna Batoni,[1] Mario Campa,[1]
Roland Brosch[4] and Semih Esin[1]**

[1]*Dipartimento di Patologia Sperimentale, Biotecnologie Mediche, Infettivologia ed Epidemiologia, University of Pisa, Pisa, Italy.*
[2]*Institut Pasteur, Unité de Régulation Immunitaire et Vaccinologie, Paris F-75015, France.*
[3]*INSERM U1041, Paris F-75015, France.*
[4]*Institut Pasteur, Unité de Pathogénomique Mycobactérienne Intégrée, Paris F-75015, France.*
[5]*VU University Medical Centre, Amsterdam, the Netherlands.*
[6]*Aeras, Rockville, MD, USA.*

Summary

The chromosome of *Mycobacterium tuberculosis* encodes five type VII secretion systems (ESX-1–ESX-5). While the role of the ESX-1 and ESX-3 systems in *M. tuberculosis* has been elucidated, predictions for the function of the ESX-5 system came from data obtained in *Mycobacterium marinum*, where it transports PPE and PE_PGRS proteins and modulates innate immune responses. To define the role of the ESX-5 system in *M. tuberculosis*, in this study, we have constructed five *M. tuberculosis* H37Rv ESX-5 knockout/deletion mutants, inactivating *eccA₅*, *eccD₅*, *rv1794* and *esxM* genes or the *ppe25-pe19* region. Whereas the Mtb*rv1794*ko displayed no obvious phenotype, the other four mutants showed defects in secretion of the ESX-5-encoded EsxN and PPE41, a representative member of the large PPE protein family. Strikingly, the Mtb*eccD₅*ko mutant also showed enhanced sensitivity to detergents and hydrophilic antibiotics. When the virulence of the five mutants was evaluated, the Mtb*eccD₅*ko and Mtb∆*ppe25-pe19* mutants were found attenuated both in macrophages

and in the severe combined immune-deficient mouse infection model. Altogether these findings indicate an essential role of ESX-5 for transport of PPE proteins, cell wall integrity and full virulence of *M. tuberculosis*, thereby opening interesting new perspectives for the study of this human pathogen.

Introduction

Mycobacterium tuberculosis, the etiological agent of human tuberculosis, employs distinct pathways that mediate protein transport across the complex mycobacterial cell envelope (Bitter *et al.*, 2009): (i) the SecA1-operated pathway, responsible for the secretion of proteins carrying typical N-terminal signal sequences, and an alternative SecA2-operated pathway for proteins lacking such sequences; (ii) the twin arginine translocation (TAT) system, devoted to the secretion of proteins with atypical N-terminal signal sequences containing two arginine residues; and (iii) the recently described type VII secretion pathway, known to secrete Esx proteins with characteristic WXG100 motifs (Pallen, 2002).

The genome of *M. tuberculosis* harbours five gene clusters coding for type VII secretion systems, designated ESX-1–ESX-5 (Cole *et al.*, 1998; Tekaia *et al.*, 1999). ESX-1 is the most extensively studied, due to its crucial implication in virulence of pathogenic mycobacteria mediated by secretion of effector molecules such as EsxA (6 kDa Early Secreted Antigenic Target, ESAT-6), its protein partner EsxB (10 kDa Culture Filtrate Protein, CFP-10), as well as EspA and other associated proteins (Pym *et al.*, 2003; Fortune *et al.*, 2005; MacGurn *et al.*, 2005; McLaughlin *et al.*, 2007; Frigui *et al.*, 2008; Gordon *et al.*, 2009; Simeone *et al.*, 2009; Garces *et al.*, 2010; Sani *et al.*, 2010; Bottai *et al.*, 2011).

In the present study we focused on the ESX-5 system, which represents the most recently evolved ESX system (Gey van Pittius *et al.*, 2001), encoded in the genomes of various slow growing mycobacteria, including the human pathogens *Mycobacterium leprae* and *Mycobacterium ulcerans* and the fish pathogen *Mycobacterium marinum*, but lacking from phylogenetically more distant saprophytic species such as *Mycobacterium smegmatis*. Similarly to
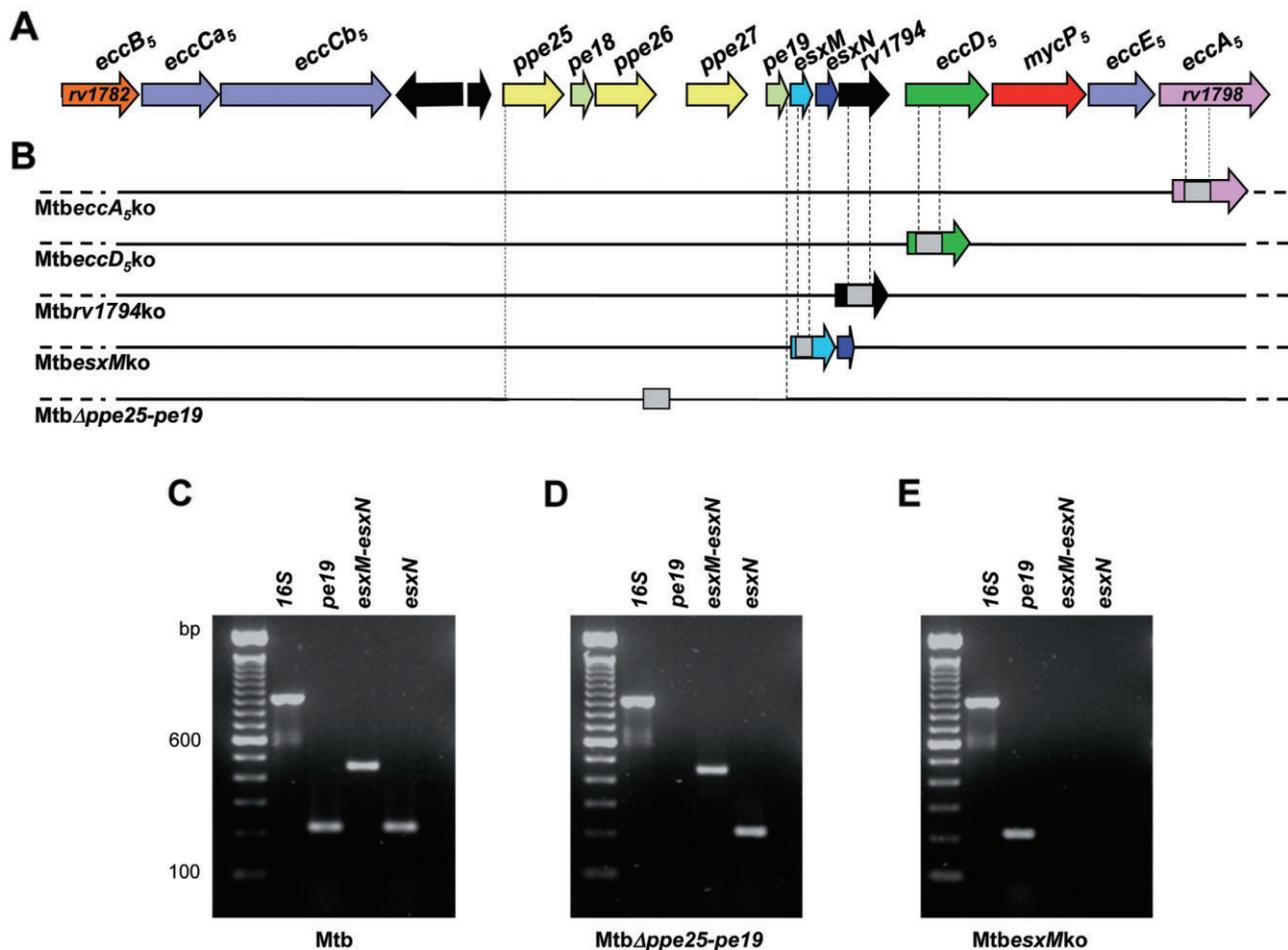
Fig. 1. Selective inactivation of ESX-5 genes in *M. tuberculosis* H37Rv.
A. Genomic organization of the ESX-5 locus in *M. tuberculosis* H37Rv. The various ESX-5 genes encoding proteins belonging to different protein families are represented by coloured arrows (Gey van Pittius *et al.*, 2006; Bitter *et al.*, 2009): orange, amino-terminal transmembrane protein; violet, amino-terminal transmembrane ATPase; yellow, PPE family; light green, PE family; light blue, CFP-10 (EsxB)-homologue; blue, ESAT-6 (EsxA)-homologue; black, *Rv1794* (orthologous to the *M. marinum* ESX-5-associated MMAR_2676 gene); green, integral membrane protein; red, mycosin (subtilisin-like serine protease); pink, AAA+ ATPase. Black arrows indicate region-associated genes coding for proteins not thought to be involved in the ESX-5 secretion machinery.
B. Schematic representation of genomic organization of ESX-5 mutants. In each mutant strain, only the arrow representing the mutated gene is depicted. The grey boxes represent the kanamycin resistance cassettes used to inactivate the various ESX-5 genes.
C–E. Analysis of *esxM–esxN* expression in WT *M. tuberculosis* (C), Mtb*Δppe25-pe19* (D) and Mtb*esxM*ko (E) mutants by RT-PCR using various combinations of primers specific for *esxM* and *esxN*. As control, RT-PCR was performed with primers specific for rRNA 16S or *pe19*.

other ESX clusters, the ESX-5 locus consists of a pair of *esx* genes (Fig. 1A), coding for EsxM and EsxN proteins, immunodominant antigens, which induce strong CD4+ T-cell responses both in humans and in different animal models (Alderson *et al.*, 2000; Jones *et al.*, 2010). Immediately upstream of *esxM/esxN* the ESX-5 locus harbours the *ppe25-pe19* gene cluster, coding for members of mycobacteria-specific protein families, named after the conserved N-terminal proline-glutamic acid (PE) or proline-proline-glutamic acid (PPE) motifs (Cole *et al.*, 1998; Tekaia *et al.*, 1999). The *ppe-pe-esx* genes are flanked by blocks of *ecc* (esx conserved components) genes that encode membrane proteins and ATP-binding proteins, predicted to be components of an ATP-powered secretion machine involved in the export of the corresponding Esx proteins (Brodin *et al.*, 2004; Bitter *et al.*, 2009). First insights into the role of ESX-5 were gained in the last few years by using *M. marinum* as model (Abdallah *et al.*, 2006; 2009; Daleke *et al.*, 2011; Weerdenburg *et al.*, 2012). Analysis of secretomes of two *M. marinum* ESX-5 transposon mutants revealed that a functional ESX-5 system is required for secretion/transport of various PPE and PE proteins, such as the heterogeneously expressed PPE41 protein from *M. tuberculosis* (Abdallah *et al.*, 2006) or PPE and PE proteins belonging to the PPE_MPTR and PE_PGRS subgroups (Abdallah *et al.*, 2009). PPE_MPTR and PE_PGRS, characterized by C-terminal domains contain-

ing Major Polymorphic Tandem Repeats (PPE_MPTR) or a Polymorphic GC-Rich Sequence (PE_PGRS), are the phylogenetically most recent subclasses of PE and PPE proteins, whose massive expansion is closely associated with the ESX-5 cluster (Gey van Pittius *et al.*, 2006). Recently, also the *M. tuberculosis* LipY lipase (LipY$_{Mt}$) and its orthologous protein in *M. marinum* (LipY$_{Mm}$) were found to be targeted to the cell surface of *M. marinum* in an ESX-5-dependent manner (Daleke *et al.*, 2011). Due to its role in the transport of PE and PPE proteins in *M. marinum*, ESX-5 is predicted to play a major role in the interaction of pathogenic mycobacteria with the host. Although the exact function of most of PPE and PE proteins is still unknown, several of these proteins have been proposed to be virulence factors (Ramakrishnan *et al.*, 2000; Brennan *et al.*, 2001; Li *et al.*, 2005). Because of their abundance (*pe* and *ppe* genes account for 7.1% of the coding capacity of the *M. tuberculosis* genome) (Cole *et al.*, 1998), their surface localization (Sampson *et al.*, 2001; Banu *et al.*, 2002; Cascioferro *et al.*, 2007; Song *et al.*, 2008; Chaturvedi *et al.*, 2010) and the highly polymorphic nature of the C-terminal domain, PPE and PE proteins are thought to be implicated in antigenic variation of mycobacterial strains (Delogu and Brennan, 2001; Bottai and Brosch, 2009).

In contrast to *M. marinum*, the biological function of the ESX-5 system in *M. tuberculosis*, as well as the impact of this system in virulence and host-pathogen interaction remain largely unknown. In the present study, in order to identify the elements constituting the *M. tuberculosis* ESX-5 secretion machinery, and to evaluate their involvement in PPE/PE transport and virulence, various genes from the ESX-5 locus were inactivated or deleted in *M. tuberculosis* H37Rv. The mutants were then tested *in vitro* for their ability to secrete EsxN and export various PPE and PE proteins, such as PPE41 and PE_PGRS proteins. Moreover, to investigate the impact of different ESX-5 genes on virulence of *M. tuberculosis*, the growth properties of all ESX-5 mutants were analysed in *ex vivo*/*in vivo* models, i.e. murine macrophages and severe combined immune-deficient (SCID) mice. This approach allowed us to characterize the ESX-5 system of *M. tuberculosis* H37Rv and demonstrate the importance of this system for the transport of particular ESX and PPE proteins and full virulence of the pathogen.

Results

Identification of ESX-5 genes required for EsxN secretion in M. tuberculosis

Five *M. tuberculosis* H37Rv knockout (KO) mutants were constructed, in which selected ESX-5 genes were inactivated by insertion of a kanamycin resistance cassette, or from which a defined genomic segment of the ESX-5

locus was deleted (Fig. 1B). Mtb*eccA$_5$*ko and Mtb*eccD$_5$*ko are inactivated for *eccA$_{5Mt}$* (*rv1798*) or *eccD$_{5Mt}$* (*rv1795*), which code for an AAA+ ATPase (EccA$_5$) or a putative transmembrane protein (EccD$_5$) of the ESX-5 secretion machinery respectively. In the Mtb*rv1794*ko strain, gene *rv1794* is interrupted, whose orthologue in *M. marinum* (MMAR_2676) encodes a protein with unknown function involved in ESX-5-linked secretion (Abdallah *et al.*, 2009). In Mtb*esxM*ko, gene *esxM* (*rv1792*) is inactivated, which is encoding a WXG-100 member in the ESX-5 region. Finally, MtbΔ*ppe25-pe19* is lacking the genomic segment containing the ESX-5-associated *ppe25-pe19* (*rv1787–rv1791*) genes. For each mutant, a complemented derivative was constructed, in which the cosmid I104, carrying the entire ESX-5 cluster, was stably integrated into the chromosome via the *attB* site, following a strategy that has previously allowed to successfully complement ESX-related mutant strains (Pym *et al.*, 2003; Brodin *et al.*, 2010; Bottai *et al.*, 2011). Southern hybridization patterns displayed by *M. tuberculosis* wild-type (WT), KO constructs and complemented strains confirmed the partial replacement of the selected ESX-5 genes by a kanamycin cassette in the different mutants as well as the presence of an intact ESX-5 cluster in complemented strains (Fig. S1).

Expression studies by reverse-transcription PCR (RT-PCR) on RNAs obtained from WT and ESX-5 mutant strains (Fig. 1C–E) demonstrated that the *esxM* gene is co-transcribed with the paired gene *esxN* (Fig. 1C). As expected, inactivation of other ESX-5 genes, such as *rv1794*, *eccD$_{5Mt}$* and *eccA$_{5Mt}$*, did not affect expression of *esxM/N* (data not shown). The *esxM/N* genes were still transcribed in the MtbΔ*ppe25-pe19* strain (Fig. 1D), indicating that ESX-5-associated *pe* and *ppe* genes are not required for the expression of downstream *esxM/N* genes. In contrast, the disruption of *esxM* also abolished the *esxN* transcription (Fig. 1E), thus indicating that the Mtb*esxM*ko strain is actually a double KO strain for the two *esx* genes encoded by the ESX-5 locus, similar as what was observed for the *esxB/A* couple of the ESX-1 system (Brodin *et al.*, 2006).

To investigate whether selected *M. tuberculosis* ESX-5 KO mutants displayed a defect in EsxN secretion, culture filtrates as well as total lysates from WT, ESX-5 KO and complemented strains were tested in Western blot analyses using an anti-EsxN polyclonal serum. As shown in Fig. 2A, large amounts of EsxN were detected in the culture filtrates as well as in total lysates of *M. tuberculosis* H37Rv WT and the Mtb*rv1794*ko mutant. Lysis controls using antibodies against GroEL2 demonstrated that these samples were not contaminated with cytosolic or membrane associated proteins, thus indicating that in contrast to its *M. marinum* orthologue, Rv1794 is not directly involved in EsxN secretion in *M. tuberculosis*. Conversely,
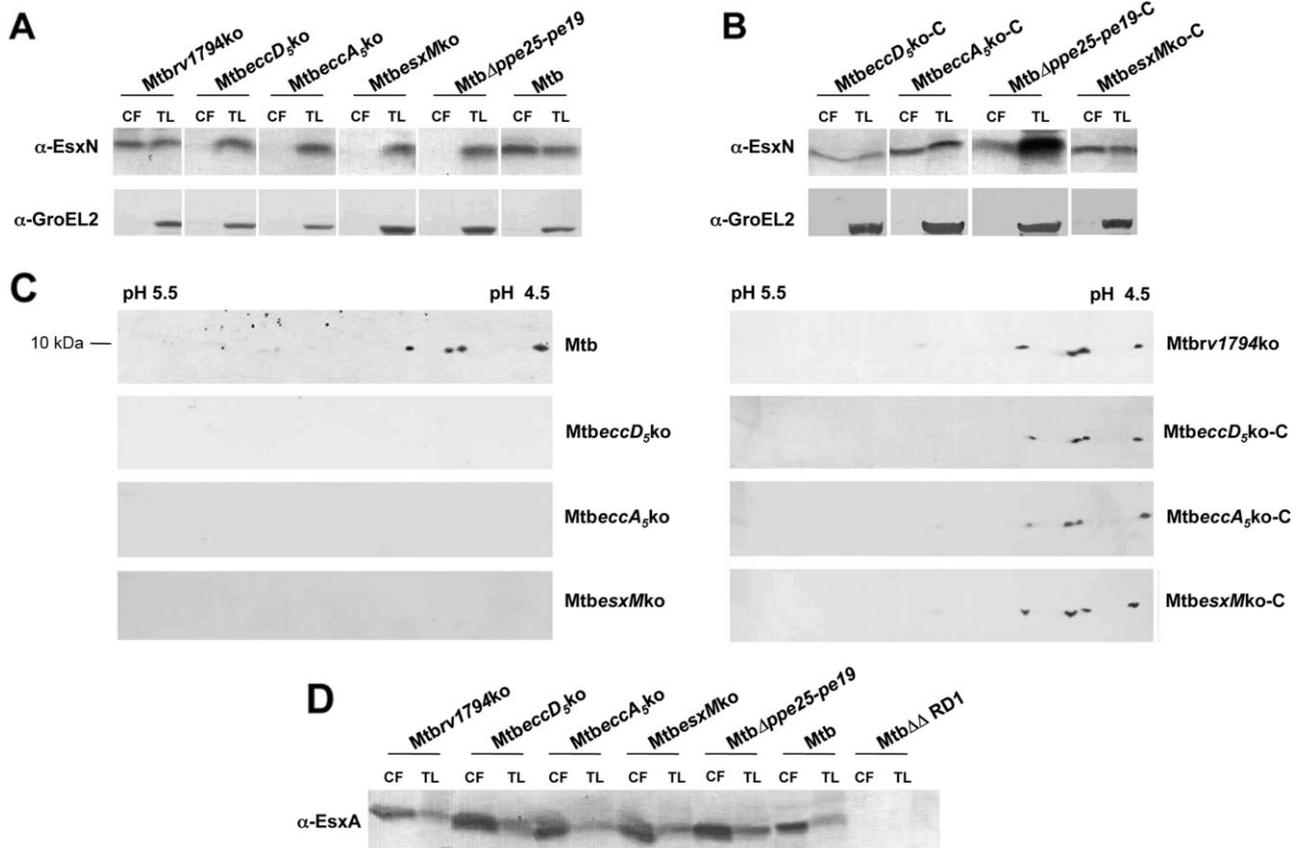
Fig. 2. *In vitro* expression and secretion of EsxN in *M. tuberculosis* ESX-5 mutants.
A and B. Fifteen micrograms of culture filtrate (CF) or total cell lysate (TL) proteins from ESX-5 mutants (A) and their complemented derivatives (B) were subjected to SDS-PAGE and tested in Western blotting by using a rabbit anti-EsxN polyclonal serum. Mouse anti-GroEL2 antibody was used for lysis control.
C. Two-dimensional analysis and immunoblot of CF from *M. tuberculosis* WT, ESX-5 KO and complemented strains. Fifty micrograms of culture supernatants were separated by isofocusing using a pH 4.5–5.5 gradient and 4–20% SDS-PAGE, in the first and second dimension respectively. Protein detection was carried out by immunoblot using the anti-EsxN polyclonal serum as previously described. For simplicity, only the region of the filter containing the anti-EsxN-recognized spots is shown.
D. Expression and secretion of EsxA in ESX-5 mutant strains. CF and TL proteins from WT *M. tuberculosis* and ESX-5 mutants were subjected to SDS-PAGE and tested in Western blot using the anti-ESAT-6 Hyb76-8 monoclonal antibody. As depicted in A, culture filtrates were negative for GroEL2. Preparations from the MtbΔΔRD1 strain were included in the immunoblotting analysis as negative control.

no EsxN was detected in the culture supernatants from MtbeccD₅ko and MtbeccA₅ko mutants, despite a 10 kDa specific band corresponding to EsxN observed in the total lysates from both these strains (Fig. 2A). These results indicate that *eccD5Mt* and *eccA5Mt* are required for an efficient translocation of EsxN. Interestingly, no EsxN specific band was detected in the culture supernatants from the MtbΔppe25-pe19 strain, suggesting that ESX-5-associated -PPE and -PE proteins also play a role in the export of this protein. In contrast to expression studies, showing a tight link between *esxM* and *esxN* expression (Fig. 1), a 10 kDa band was recognized by the anti-EsxN polyclonal serum in the total lysates from the MtbesxMko mutant. The *M. tuberculosis* genome harbours four other *esxN*-like genes not associated to any ESX cluster (Cole *et al.*, 1998; Uplekar *et al.*, 2011), which are co-transcribed with their paired *esxM*-like genes during the *in vitro* growth

(data not shown). EsxN and the four EsxN-like proteins, collectively known as Mtb9.9 family (Alderson *et al.*, 2000), share highly similar protein sequence, differing only by a few amino acids. When immunoblot analysis was performed on culture supernatants subjected to 2D gel electrophoresis, four different spots were detected in the culture supernatants from the WT strain as well as from the Mtb*rv1794*ko mutant (Fig. 2C). The absence of specific spots recognized by the anti-EsxN serum in the culture filtrates from the KO mutants suggests that ESX-5 is involved in the secretion of all Mtb9.9 proteins and that secretion of EsxN and/or EsxM is required for secretion of other Mtb9.9 family members. However, the exact identification by mass spectrometry of the four spots recognized by the anti-EsxN serum was unsuccessful, due to low amount of the proteins. For this reason, it cannot be excluded that some spots might represent different iso-
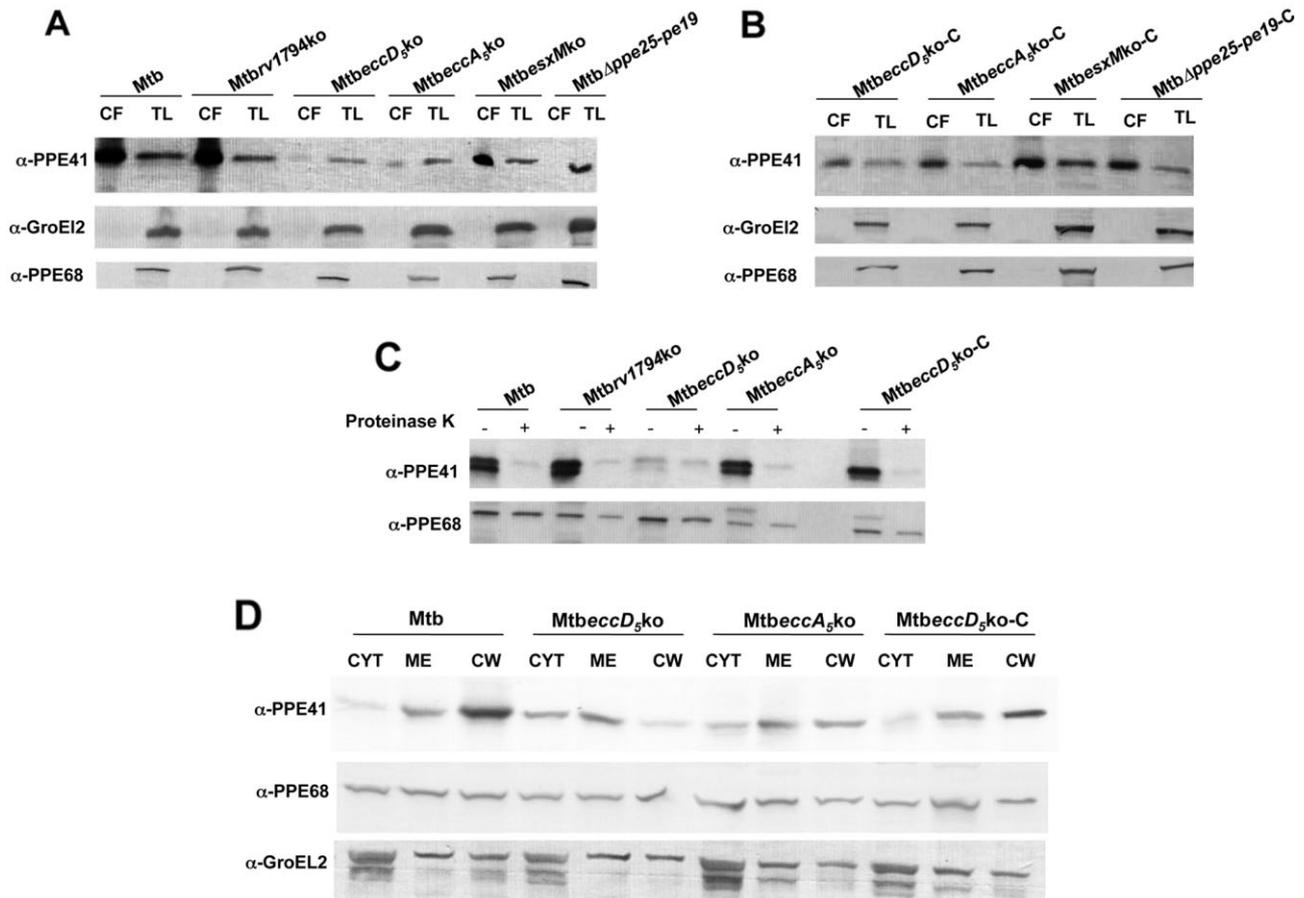
Fig. 3. Effect of ESX-5 inactivation on PPE41 secretion and transport.
A and B. Culture supernatants and total lysates from WT *M. tuberculosis* and ESX-5 mutants (A) or complemented strains (B) were tested in Western blot with anti-PPE41 rabbit polyclonal serum. As control, samples were tested with a mouse anti-GroEL2 antibody or a rabbit polyclonal serum anti-PPE68.
C. Proteinase K sensitivity assay performed on WT *M. tuberculosis*, Mtb*rv1794*ko, Mtb*eccD₅*ko and Mtb*eccA₅*ko. Live bacteria were incubated with (+) or without (−) proteinase K, and the whole cell lysates obtained from treated and untreated bacteria were separated by SDS-PAGE. PPE41 and PPE68 detection was carried out by immunoblotting as previously reported.
D. Ten micrograms of cytoplasm (CYT), membrane (ME) and cell wall (CW) proteins from WT *M. tuberculosis*, Mtb*eccD₅*ko and Mtb*eccA₅*ko strains were tested in Western blot using anti-PPE41 and anti-PPE68 polyclonal sera.

forms of EsxN, resulting from post-transcriptional modifications. As depicted in Fig. 2B and C, secretion of EsxN was restored in all complemented strains.

Preliminary experiments in *M. marinum* suggested a potential cross-interaction between ESX-1 and ESX-5 (A. Abdallah and W. Bitter, unpubl. obs.). To investigate whether the inactivation of ESX-5 could affect the secretion of ESX-1 substrates, culture filtrates from all ESX-5 mutants were tested in Western blotting for the presence of EsxA (ESAT-6). Whereas no EsxA was observed in culture filtrates from the negative control strain MtbΔΔRD1 (Bottai *et al.*, 2011) (Fig. 2D), similar amounts of the protein were detected in samples from various ESX-5 mutants and WT *M. tuberculosis* (Fig. 2D), suggesting that the inactivation of different components of the ESX-5 secretion apparatus has no relevant impact on EsxA production and secretion.

PPE41 and PE_PGRS secretion/transport in ESX-5 mutant strains

Previous findings in *M. marinum* showed that various PPE and PE proteins, such as PPE41 and PE_PGRS, are exported in an ESX-5-dependent manner (Abdallah *et al.*, 2006; 2009). In order to investigate whether these proteins were secreted/transported via the ESX-5 system also in *M. tuberculosis*, all ESX-5 mutants, their complemented derivatives and the WT strain were tested for their ability to secrete PPE41 and PE_PGRS proteins in the same growth conditions that have been previously described for *M. marinum* ESX-5 mutants using Middlebrook 7H9 medium (Abdallah *et al.*, 2006; 2009). As shown in Fig. 3A, a specific band of 23 kDa corresponding to PPE41 was observed in culture supernatants from

the *M. tuberculosis* control strain as well as in preparations from Mtb*rv1794*ko and Mtb*esxM*ko strains. PPE41 was still detected in the culture supernatants from the Mtb*eccA₅*ko mutant, although the amounts were substantially lower than those detected in samples from the WT strain. In contrast, a clear defect in PPE41 secretion was observed for Mtb*eccD₅*ko: no specific band corresponding to PPE41 was indeed detected in the culture supernatants from this strain, despite the presence of a PPE41-specific band in the whole cell lysates. Similarly, no PPE41 was detected in culture filtrates from Mtb*Δppe25-pe19*, further suggesting that ESX-5 encoded PE and PPE proteins might be involved in the ESX-5 secretion machinery. Secretion of PPE41 in culture supernatants was restored in Mtb*eccD₅*ko-C and Mtb*Δppe25-pe19*-C complemented strains (Fig. 3B).

When samples were tested with the anti-PGRS antibody, a few PE_PGRS proteins were observed in the culture filtrates of *M. tuberculosis* H37Rv. However, although some differences in the amounts of PE_PGRS proteins were detected in culture filtrates from various ESX-5 KO and complemented strains (Fig. S2), variations in the protein pattern recognized by the anti-PGRS antibody appeared to be weaker than differences previously observed in ESX-5 *M. marinum* mutants (Abdallah *et al.*, 2009). No significant difference was detected among the strains when the analysis of PE_PGRS secretion was performed on culture supernatants obtained from bacteria grown in Sauton medium (data not shown). The lack of GroEL2 and PPE68 in culture supernatants from all tested strains confirmed the absence of contamination of these samples with cell-associated proteins (Fig. 3A and B).

To investigate more in-depth the impact of *eccD₅Mt* inactivation on transport of PPE41 and PE_PGRS, the localization of these proteins was determined both in WT and Mtb*eccD₅*ko strains as well as in Mtb*rv1794*ko and Mtb*eccA₅*ko mutants by proteinase K assays and Western blot analysis of subcellular fractions. As control, the localization of PPE68 was analysed. The proteinase K treatment removed the majority of PPE41 in *M. tuberculosis* WT, Mtb*rv1794*ko and Mtb*eccA₅*ko (Fig. 3C), indicating that in these strains the protein is exposed on the bacterial surface. In contrast, the protein was (partially) resistant to the protease treatment in the Mtb*eccD₅*ko mutant, suggesting that PPE41 is not exposed on the cell surface of this strain. Western blot analysis of cytosol, membrane and cell wall fractions with the anti-PPE41 antibody demonstrated that the protein was mainly associated to membrane and cell wall in the WT *M. tuberculosis* strain and Mtb*eccA₅*ko mutant. In contrast, the protein accumulated in the cytoplasm and membrane fractions in Mtb*eccD₅*ko (Fig. 3D), further confirming an involvement of EccD₅ in the transport of PPE41. These analyses revealed substantially lower amounts of PPE41 in the Mtb*eccD₅*ko mutant as compared to the control strain. It cannot be excluded that the protein might have a reduced stability as consequence of its altered localization. Sensitivity to proteinase K treatment and translocation to cell wall were restored in the Mtb*eccD₅*ko-C complemented derivative (Fig. 3C and D).

Western blot analysis of proteinase-K-treated sample from WT *M. tuberculosis* H37Rv with the anti-PGRS monoclonal antibody revealed that some PE_PGRS proteins were sensitive to protease digestion and thus exposed to the mycobacterial surface (data not shown). In agreement with data from secretion analyses, PE_PGRS protein patterns from proteinase K-treated WT *M. tuberculosis* H37Rv and ESX-5 mutants revealed no appreciable differences between WT and mutant strains (data not shown). Similarly as what was observed in samples from WT *M. tuberculosis*, PPE68 was resistant to protease treatment and efficiently translocated to membrane and cell wall also in the Mtb*eccD₅*ko mutant (Fig. 3C and D), thus suggesting that this ESX-1-associated protein is not exposed on the mycobacterial surface and is transported to the cell wall in an ESX-5-independent manner. Together, these results indicate that in *M. tuberculosis*, a functional ESX-5 system is required for an efficient translocation and a correct localization of PPE41.

Effect of ESX-5 inactivation on cell wall integrity

To investigate the impact of ESX-5 inactivation on cell wall integrity/stability, the survival of the Mtb*eccD₅*ko and WT *M. tuberculosis* after exposure to detergents was compared. Bacteria in logarithmic growth phase were exposed to 0.1% SDS treatment and after 6 h viable bacteria were counted. Although the addition of the detergent caused a rapid decrease in the cfu numbers recovered for all the tested strains (Fig. 4A), the Mtb*eccD₅*ko mutant showed an enhanced sensitivity to SDS as compared to control strains: the percentage survival values were 1% for the Mtb*eccD₅*ko mutant and 10% for the WT or the complemented Mtb*eccD₅*ko-C strains respectively (Fig. 4B). The greater sensitivity of the Mtb*eccD₅*ko mutant to SDS was confirmed when bacterial survival was assessed after 24 and 72 h of incubation with SDS (data not shown). The sensitivity of the other ESX-5 KO strains was comparable to that of the parental strain (Fig. 4).

The mycobacterial cell envelope, which represents an effective barrier to both hydrophobic and hydrophilic solutes, is considered a major determinant of the intrinsic resistance of *M. tuberculosis* to different antibiotics (Brennan and Nikaido, 1995). Thus, alterations in cell wall integrity may also be detected by measuring the susceptibility of mycobacteria to various antibiotics. To further evaluate the effects of *eccD₅Mt* inactivation on cell wall properties, the susceptibility of Mtb*eccD₅*ko, WT *M. tuberculosis* and other ESX-5 mutants (e.g. Mtb*Δppe25-pe19*)
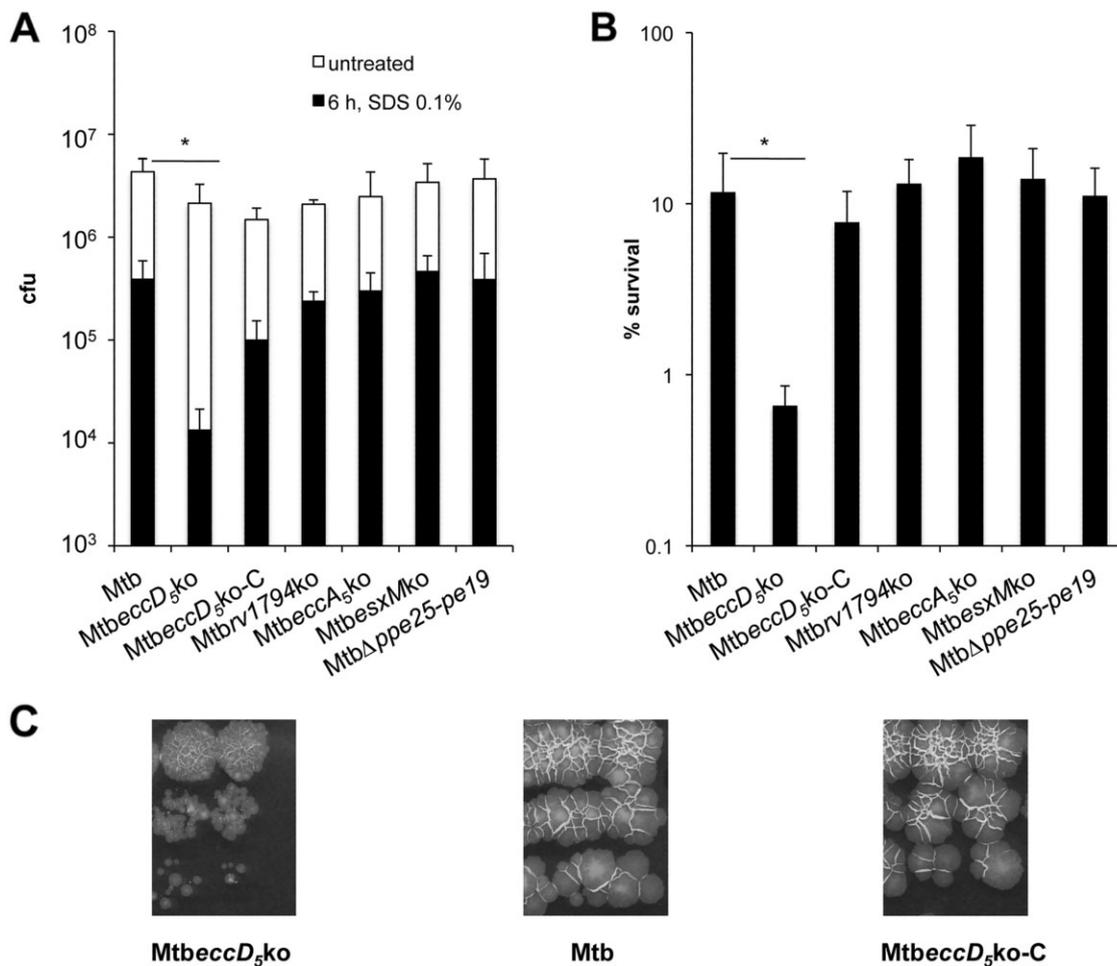
Fig. 4. Effect of EccD$_5$ disruption on cell wall integrity of *M. tuberculosis*.
A and B. Sensitivity of Mtb*eccD$_5$*ko and other ESX-5 mutants to SDS. Bacterial strains were exposed to SDS 0.1% for 6 h and the number of cfu (A) and the survival percentages (B) were determined. The means and the standard deviations of cfu values and survival percentages obtained in four independent experiments are shown. The significant difference in cfu and survival percentage values between H37Rv and Mtb*eccD$_5$*ko strain was determined by one-way ANOVA test, followed by Bonferroni post-hoc test (*$P < 0.05$).
C. Growth of Mtb*eccD$_5$*ko on solid medium. Three-week-old cultures of Mtb*eccD$_5$*ko, *M. tuberculosis* WT and the Mtb*eccD$_5$*ko-C strain grown on Middlebrook 7H11 medium. Bacterial cultures were washed, resuspended and serially 10-fold diluted in PBS: a sample of 20 µl of each dilution was spotted onto agar plates.

to various classes of antibiotics with diverse chemical structure and mechanism of action to which mycobacteria are naturally resistant was compared (Jackson *et al.*, 1999). These included antibiotics targeting several steps in the cell wall biosynthetic pathway, such as ampicillin, bacitracin and vancomycin; antibiotics targeting DNA replication such as ofloxacin and norfloxacin; antibiotics targeting transcription, such as rifampicin, which is also a front-line anti-tuberculosis drug. Isoniazid and ethambutol, two antibiotics affecting the cell wall biosynthesis, to which mycobacteria are susceptible, were included in the analysis for control purposes. As shown in Table 1, while all strains displayed comparable sensitivity to isoniazid and ethambutol, the Mtb*eccD$_5$*ko mutant was highly sensitive to ampicillin, vancomycin and bacitracin. The MIC values for these antibiotics were indeed 32- or 64-fold lower for the

Table 1. Drug sensitivity of Mtb*eccD$_5$*ko mutant.

	Mtb*eccD$_5$*ko	Mtb	Mtb*eccD$_5$*ko-C
Ampicillin (µg ml^{-1})	12.5	400	n.a.
Bacitracin (µg ml^{-1})	6.25	400	400
Vancomycin (µg ml^{-1})	1.25	>40	10
Norfloxacin (µg ml^{-1})	1.25	2.5	2.5
Ofloxacin (µg ml^{-1})	0.125	1	0.5
Rifampicin (µg ml^{-1})	0.03	0.06	0.06
Isoniazid (µg ml^{-1})	0.5	0.5	0.5
Ethambutol (µg ml^{-1})	3.2	3.2	3.2

MIC values were determined as the lowest concentration of antibiotic which reduced the bacterial viability by at least 99% on solid medium. n.a.: not applicable due to the presence of an ampicillin resistance gene in the cosmid used for the construction of the complemented strain.
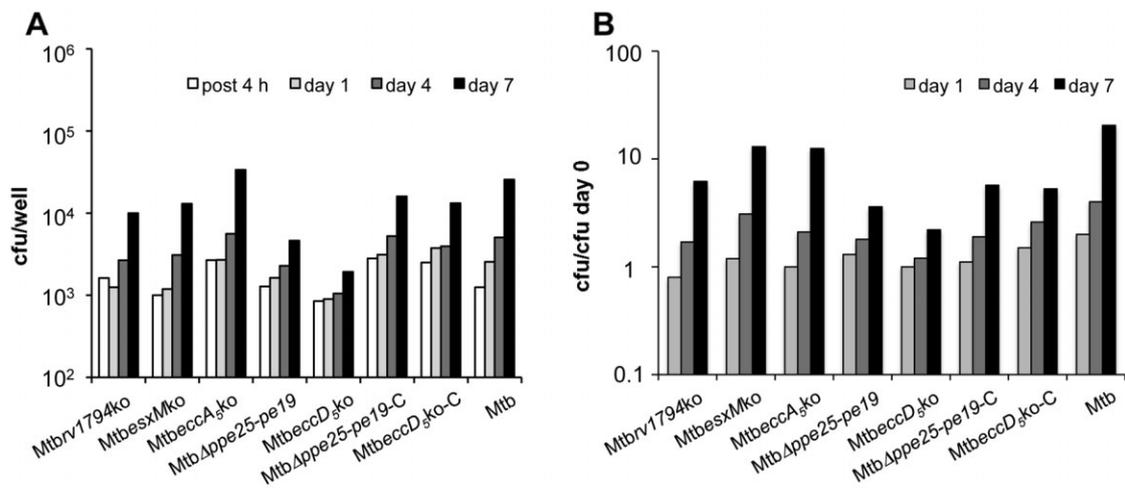
Fig. 5. Intracellular growth of ESX-5 mutant strains in BMDM. BMDM (1×10^4 cells per well) obtained from C57BL/6 mice were infected with various ESX-5 mutants, their corresponding complemented derivatives, and the WT *M. tuberculosis* H37Rv strain using an moi of 1:1. cfu numbers of intracellular bacteria were determined 4 h, and 1, 4 and 7 days after infection. The figure shows the average of cfu numbers (A) and fold growth values (cfu/cfu at day 0) (B) obtained in one experiment performed in triplicate.

Mtb*eccD5*ko mutant than those of the WT strain (Table 1) or the MtbΔ*ppe25-pe19* mutant (data not shown). The enhanced sensitivity of the Mtb*eccD5*ko strain to hydrophilic antibiotics was confirmed when the susceptibility was tested by using the microplate-based nitrate reductase assay in broth (Kumar *et al.*, 2005). In this case, the MIC values for ampicillin, vancomycin and bacitracin were 0.25, 0.5 and 8 μg ml^{-1} for Mtb*eccD5*ko and 100, 8 and 256 μg ml^{-1} for the WT *M. tuberculosis* H37Rv or MtbΔ*ppe25-pe19* respectively. These results thus suggest that the inactivation of the ESX-5 system via the disruption of EccD5 strongly affects the mutant's cell wall stability. This effect was also visible by inspection of the Mtb*eccD5*ko mutant on Middlebrook 7H11 plates, which was characterized by a small colony phenotype that was reverted upon complementation with the cosmid encoding a functional ESX-5 system (Fig. 4B). It is noteworthy that the Mtb*eccD5*ko strain also displayed smaller colonies than the *M. tuberculosis* H37Rv control on Middlebrook 7H9 agar plates without malachite green (data not shown), thus suggesting that the small colony morphotype of the EccD5 mutant is not due to the presence of this inhibitory agent in the medium. The finding that the Mtb*eccD5*ko mutant showed no difference in growth as compared to the WT strain in liquid medium (Fig. S3) further emphasizes the importance of EccD5 and ESX-5 in general for a fully functional cell envelope that determines the contact with its immediate environment.

Growth of the ESX-5 mutant strains in macrophages

To investigate the effect of ESX-5 inactivation on intracellular growth characteristics of *M. tuberculosis*, the *ex vivo* growth of the ESX-5 mutants and the WT strain were compared in bone marrow-derived macrophages (BMDM). Cells were infected with the various strains at a multiplicity of infection (moi) of 1:1, and the number of intracellular bacteria was determined at 4 h, and 1, 4 and 7 days after infection. The ESX-5 mutants were taken up by BMDM with similar efficiency as the *M. tuberculosis* WT (data not shown), indicating that inactivation of different components of the ESX-5 system has no relevant impact on the ability of *M. tuberculosis* to be engulfed by host macrophages.

In contrast, when the *ex vivo* growth kinetics of the various ESX-5 KO strains were analysed, differences in their intracellular growth abilities were observed (Fig. 5). The Mtb*rv1794*ko, Mtb*esxM*ko and Mtb*eccA5*ko mutants showed intracellular growth kinetics similar to that of the *M. tuberculosis* WT, resulting in 1 log$_{10}$ increase in the cfu number over a 7 day period. It should be mentioned, however, that the Mtb*eccA5*ko showed impaired growth as compared to the WT *M. tuberculosis* H37Rv in THP-1-derived macrophages and type II pneumocyte cell line (A549) (Fig. S4). An attenuated phenotype in murine macrophages was observed for MtbΔ*ppe25-pe19* and Mtb*eccD5*ko mutants. Seven days after infection, only a 0.5 log$_{10}$ increase was indeed observed in the cfu numbers recovered from macrophages infected with this mutant strain MtbΔ*ppe25-pe19*. An even stronger attenuation phenotype was displayed by the Mtb*eccD5*ko mutant for which no growth was observed in murine macrophages over the same period. Complementation of MtbΔ*ppe25-pe19* and Mtb*eccD5*ko strains with an entire ESX-5 cluster increased the intracellular growth ability of the mutants, resulting in a 0.8 log$_{10}$ increase in the cfu numbers recovered from infected cells after 7 days from infection.
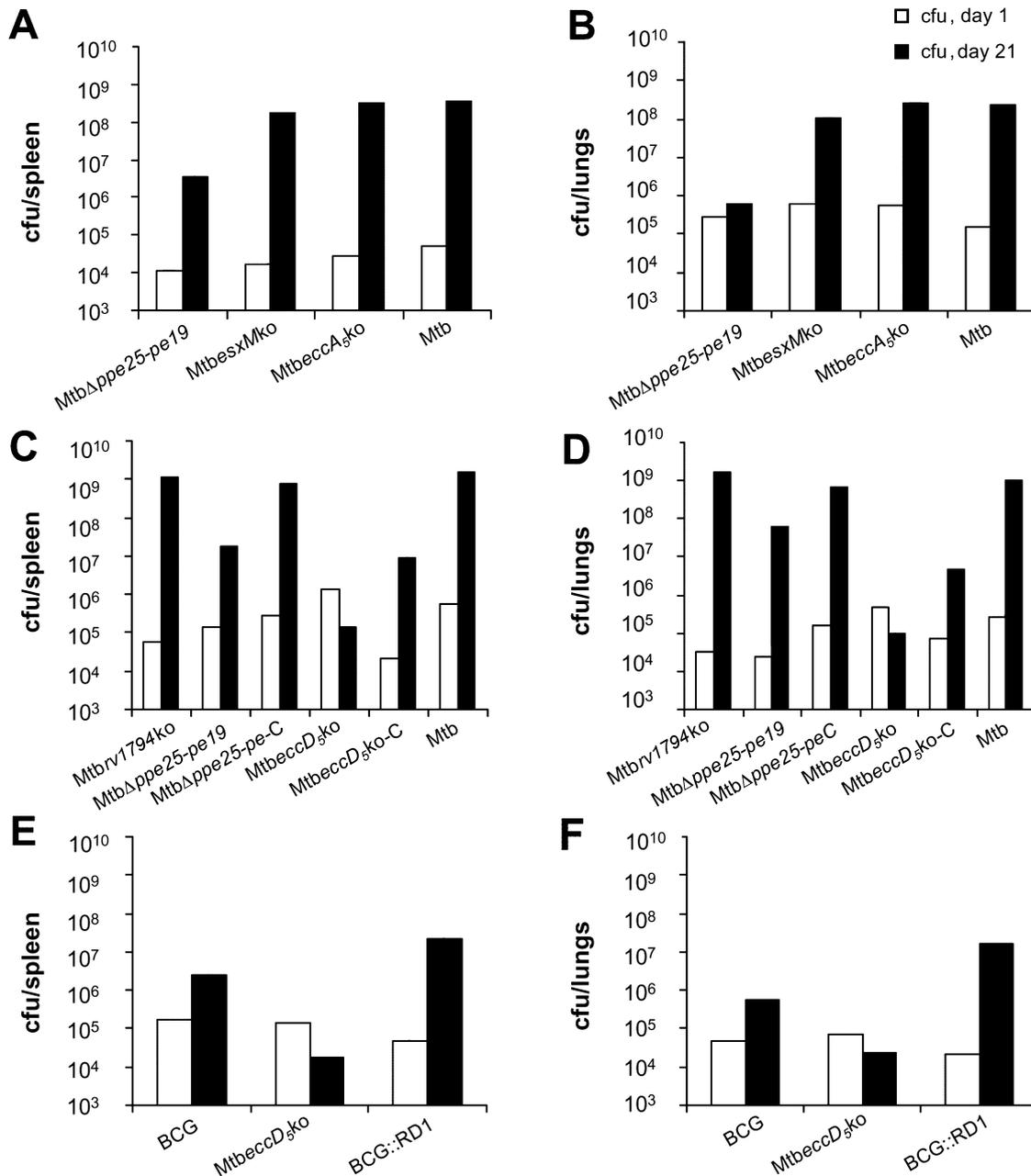
Fig. 6. Virulence of different ESX-5 mutant strains in a SCID mouse infection model. SCID mice were infected intravenously with 1×10^6 cfu per mouse of various ESX-5 mutant and control strains. A, C and E depict the average cfu numbers recovered from the spleen of groups of three to four mice in three independent experiments at day 1 and day 21 post infection. B, D and F show the average cfu numbers in the lungs of the same groups of mice.

Virulence of the ESX-5 mutants in SCID mice

The impact of ESX-5 inactivation on virulence of *M. tuberculosis* was assessed by evaluating the *in vivo* growth of ESX-5 mutants in SCID mice. In agreement with results obtained from murine macrophage infection studies, the Mtb*eccA₅*ko, Mtb*esxM*ko and Mtb*rv1794*ko mutants displayed a rapid growth both in spleen and lungs of infected

mice (Fig. 6A–D), as indicated by high bacterial load in the target organs (10^8–10^9 cfu) and severe splenomegaly (data not shown), comparable to those observed for the *M. tuberculosis* WT.

Conversely, the MtbΔ*ppe25-pe19* mutant showed a strongly attenuated phenotype. Three weeks after infection, a 3- and 2-log$_{10}$ reduction was observed in the numbers of cfu recovered from spleen and lungs of

MtbΔ*ppe25-pe19*-infected mice relative to the *M. tuberculosis* H37Rv-infected controls (Fig. 6A–D). Levels of virulence similar to those of the *M. tuberculosis* control strain were restored in the ESX-5 complemented MtbΔ*ppe25-pe19*-C derivative (Fig. 6C and D). The Mtb*eccD$_5$*ko strain showed an even stronger attenuation: inactivation of *eccD$_{5Mt}$* gene resulted indeed in no growth either in spleen or lungs of infected mice over a 21 day period (Fig. 6C and D), and reduced splenomegaly (data not shown). Complementation of Mtb*eccD$_5$*ko with a functional ESX-5 system increased the *in vivo* growth of the strain, resulting in a 3 log$_{10}$ increase in numbers of cfu recovered in spleen and lungs, although it did not restore the virulence to the level of the WT strain.

The severe attenuation of the Mtb*eccD$_5$*ko mutant was further confirmed when the *in vivo* growth of this strain was compared to that of the vaccine strain *Mycobacterium bovis* BCG (BCG) and the partially virulent BCG::RD1 (Brodin *et al.*, 2006). As depicted in Fig. 6E and F, no growth was observed for the Mtb*eccD$_5$*ko mutant, whereas 1- and 2-log$_{10}$ increase in cfu number was observed in spleen and lungs of mice infected with BCG and BCG::RD1 strains respectively.

Discussion

The role of the ESX-5 system in the export of selected PPE and PE proteins in *M. marinum*, as well as the involvement of this system in modulation of cytokine responses by *M. marinum*-infected human macrophages are well established (Abdallah *et al.*, 2006; 2008; 2009; Daleke *et al.*, 2011). In contrast, nothing is known about the function of the ESX-5 system in *M. tuberculosis.* The present study was thus focused on the characterization of the ESX-5 system of *M. tuberculosis* on the basis of ESX-5 KO and deletion constructs.

As a first conclusion drawn from the results obtained, the characteristics of different mutants and the positions of the corresponding inactivated genes argue against the possibility that the phenotypes displayed by the various ESX-5 mutants (with exception of the *EsxM/N* couple, for which a downstream effect of *esxM* disruption on *esxN* was observed) were due to polar effects on the expression of downstream genes. Screening of ESX-5 mutants for their ability to secrete EsxN showed that *eccA$_{5Mt}$* and *eccD$_{5Mt}$* are required for secretion of EsxN. These genes are homologous to *eccA$_{1Mt}$* (*rv3868*) and *eccD$_{1Mt}$* (*rv3877*), both encoding for components of the ESX-1 secretion apparatus involved in transport of ESAT-6 and CFP-10 (Brodin *et al.*, 2006). In contrast to the ESX-1-encoded *pe35* gene that is implicated in the expression of *esxB/esxA* (Brodin *et al.*, 2006), the ESX-5-associated *pe* and *ppe* genes are dispensable for the expression of *esxM/N* but required for secretion of EsxN. Finally, *rv1794*, the

orthologue of MMAR_2676, which in *M. marinum* was reported to affect EsxN secretion and export of various PE and PPE proteins (Abdallah *et al.*, 2009), is not implicated in the secretion of EsxN in *M. tuberculosis* H37Rv. These findings suggest that in spite of high amino acid similarity (96% identity), Rv1794 and MMAR_2676 might have different functions in the ESX-5 secretion machinery that have evolved as a consequence of the adaptation of these two mycobacterial species to different hosts. Substantial differences in function of proteins encoded by ESX clusters from different mycobacterial species have been previously described for the ESX-1 secretion-associated protein EspG$_1$ (Bottai *et al.*, 2011), which shows weak similarity with Rv1794. While EspG$_{1Mm}$ is required for EsxA secretion and virulence in *M. marinum* (Gao *et al.*, 2006), the EspG$_{1Mt}$ is not directly involved in EsxA secretion, although it plays a relevant role in virulence of *M. tuberculosis* (Bottai *et al.*, 2011). Alternatively, the function of Rv1794 could be redundant in *M. tuberculosis*.

PPE41 secretion and localization studies in *M. tuberculosis* ESX-5 mutant strains confirmed previous findings in *M. marinum* showing a major role of the ESX-5 secretion system in PPE export. However, the various components of the ESX-5 secretion apparatus seem to have a different impact on this process. Whereas only minor reduction of PPE41 transport was observed after disruption of the *eccA$_{5Mt}$* gene, the inactivation of *eccD$_{5Mt}$* abolished the secretion of PPE41, and also resulted in a profound reduction of the amounts of PPE41 transported to the bacterial envelope. It is plausible that the different phenotypes exhibited by EccD$_5$ and EccA$_5$ mutants might be caused by a deviating involvement of the proteins in the stability of the ESX-5 secretion machinery. Recently, biochemical characterization of ESX-5 components in *M. marinum* and BCG suggested that EccD$_5$ is part of a four-membered protein complex forming the core of the ESX-5 secretion apparatus, whereas EccA$_5$ is not part of this complex (E. Houben, pers. comm.). Thus, disruption of a core component, such as EccD$_5$, likely abolishes the stability of the entire complex. In support of this hypothesis, preliminary immunoblotting experiments identified much lower amounts of EccB$_5$, another ESX-5 core component, in membrane and cell wall fractions of Mtb*eccD$_5$*ko relative to WT and Mtb*eccA$_5$*ko strains (Fig. S5). These results suggest that EccD$_5$ and EccB$_5$ are indeed part of the same core complex, which does not include EccA$_5$ (Fig. S5) or ESX-5-associated PE and PPE proteins (data not shown). In addition, the minor effect of *eccA$_5$* disruption in *M. tuberculosis* on PPE41 secretion compared to *M. marinum* (Abdallah *et al.*, 2006) might also be due to a possible redundancy of *eccA$_5$* with homologues *eccA* genes from other ESX systems such as ESX-2, which is not present in the genome of *M. marinum* (Stinear *et al.*, 2008). However,

as deletion of the ESX-2 cluster in the Mtb*eccA₅*ko genetic background did not interrupt the PPE41 secretion in the double mutant (data not shown), this does not seem to be the case. The example of *eccA₅*, like for *rv1794* and *espG₁*, shows again that in spite of the high conservation of ESX loci between *M. marinum* and *M. tuberculosis* certain genes might not have the same impact in one species than in the other. Finally, it cannot be excluded that other AAA+ ATPases specifically present in *M. tuberculosis* might complement for the loss of EccA₅Mt function.

No obvious effect on PE_PGRS proteins exposed on the cell surface or released in the culture supernatants was detected after inactivation of different components of the ESX-5 secretion machinery in *M. tuberculosis* H37Rv. These results are in contrast with previous observations in *M. marinum*, where several *M. marinum* specific PE_PGRS proteins are secreted in an ESX-5-dependent manner (Abdallah *et al.*, 2009). A number of studies suggest that some PE_PGRS and PPE proteins are associated with the cell envelope. It is possible that the impact of ESX-5 inactivation on release of PE_PGRS proteins is also affected by the composition of the cell wall. For example, cell wall of *M. marinum* contains a group of glycolipids, designated lipooligosaccharides (LOSs), which are absent from the cell wall of *M. tuberculosis* H37Rv and several *M. tuberculosis* clinical isolates (Ren *et al.*, 2007). As the number and composition of PE_PGRS proteins as well as their expression profiles vary considerably among different *M. tuberculosis* strains (Voskuil *et al.*, 2004), strain specific differences in PE_PGRS secretion patterns might as well occur.

Although the growth of *M. tuberculosis* in liquid medium is not affected by disruption of individual components of the ESX-5 secretion machinery (Fig. S3), the virulence properties of *M. tuberculosis* are strictly dependent on a functional ESX-5 system (Fig. 6). Disruption of *eccD₅* indeed results in the loss of the ability of *M. tuberculosis* to replicate in SCID mice. Differently from ESX-1 mutants, whose attenuation is due to defects in EsxA/B expression or secretion (Brodin *et al.*, 2006), the attenuation of the Mtb*eccD₅*ko mutant is not related to the loss of EsxN secretion. Indeed, the characterization of the *ex vivo* and *in vivo* growth properties of the Mtb*esxM*ko mutant demonstrated that inactivation of *esxM/esxN* genes does not result in attenuation of virulence of *M. tuberculosis*. The profound attenuation of virulence of *M. tuberculosis* resulting from inactivation of *eccD₅* could be in part due to the alteration of the integrity of the mycobacterial cell wall. Alteration of cell wall structure may cause attenuation of virulence by disrupting the bacterial interface with the host cell, undermining specific virulence functions, or increasing the susceptibility of the microorganism to host antimicrobial defences (Barry, 2001). Such a scenario is in good agreement with the increased sensitivity of the

Mtb*eccD₅*ko strain to detergents and antibiotics to which mycobacteria are naturally resistant. Apart from the direct implication of the EccD₅-containing multi-membered protein complex in cell envelope stability (see above), some of the observed effects might also be linked to a defect in transport of PPE proteins and/or other mycobacterial cell wall components in ESX-5 mutants. To date, the function and localization of ESX-5-associated PPE and PE proteins are unknown. However, as the virulence of the MtbΔ*ppe25-pe19* mutant was also found to be attenuated, it seems likely that these proteins, as well as their transport across the cytoplasmic membrane, might play a role for a fully functional cell envelope. Because of their high homology in primary amino acid sequence, it cannot be excluded that these PE and PPE proteins might play a redundant role in *M. tuberculosis* virulence. Homologous recombination events between *ppe25* and *ppe27* genes resulting in deletion of *ppe25*, *pe18* and *ppe26* genes have been reported in some Tunisian clinical isolates of *M. tuberculosis* (Karboul *et al.*, 2008). As these clinical isolates apparently conserved their virulence and infectivity, it is plausible that not all of the five PE and PPE proteins in the ESX-5 locus, deleted in the attenuated MtbΔ*ppe25-pe19* strain, are involved in virulence functions. However, it seems likely that at least one PE/PPE pair from the ESX-5 region is. A similar situation was observed in *M. avium*, where a PPE25 homologue is required for growth in macrophages and in mice (Li *et al.*, 2005).

In agreement with the above mentioned minor effects on PPE transport and resistance to cell wall stresses, no defect in the virulence properties of *M. tuberculosis* in SCID mice was observed after inactivation of *eccA₅*. However, it should be mentioned that the *eccA₅* gene was recently identified as required for cholesterol catabolism in *M. tuberculosis* (Griffin *et al.*, 2011). As cholesterol uptake and catabolism are not required for growth during the acute phase of infection but for mycobacterial persistence during the chronic phase (Pandey and Sassetti, 2008), it cannot be excluded that a more evident growth defect might be observed for the Mtb*eccA₅*ko mutant during long-term infection experiments. In this respect, it is also noteworthy that *eccA₅* was suggested as virulence factor in the guinea-pig infection model (Jain *et al.*, 2007). The impact of EccA₅ on *in vivo* growth of *M. tuberculosis* might thus vary with the type of infected host, which is also relevant to our observation that the Mtb*eccA₅*ko mutant strain has an impaired intracellular growth in human THP-1 and A549 cell lines (Fig. S4).

In conclusion, the results obtained in this study demonstrate that the ESX-5 system of *M. tuberculosis* has an important function for the cell wall integrity and virulence of *M. tuberculosis*. It is clear that the ESX-5 system in *M. tuberculosis* shares certain basic features with the ESX-5 system in *M. marinum* that can now be evaluated

also in other *M. tuberculosis* lineages. However, several differences have also been highlighted, which seem to be specific for the system in *M. tuberculosis*. After the ESX-1 and the ESX-3 systems of *M. tuberculosis*, which were subject of numerous publications from various research groups, our data allow new insights to be made into the ESX-5 system of *M. tuberculosis*. From comparison of the three ESX systems studied so far in *M. tuberculosis*, it is obvious that despite their different functions, each of them plays an important role in the biology and pathogenicity of the etiological agent of human tuberculosis, which makes them interesting and important targets for potential new prevention and control strategies.

Experimental procedures

Plasmids, bacterial strains and growth conditions

Plasmid pPR27, used for construction of KO strains, is a thermosensitive vector, carrying the *sacB* counterselectable marker (Pelicic *et al.*, 1997); plasmid pUC4K (Amersham Biosciences) contains the kanamycin resistance cassette (*aph*); cosmid I104, used for construction of complemented strains, is an integrative pYUB412 vector (Bange *et al.*, 1999) containing a 41 kb fragment (2005–2046 kb) of the *M. tuberculosis* H37Rv genome including the entire ESX-5 locus. For cloning procedures and plasmid amplification, *Escherichia coli* DH10B (Invitrogen) was grown either in LB liquid or solid medium, added when required with 20 µg ml⁻¹ of gentamicin, 100 µg ml⁻¹ of hygromycin or 100 µg ml⁻¹ of ampicillin. For the construction of mycobacterial KO mutants, *M. tuberculosis* H37Rv (stocks held at the Institut Pasteur) (Cole *et al.*, 1998) was used as the reference strain. *M. tuberculosis* strains were grown in Middlebrook 7H9 medium (Becton-Dickinson) supplemented with albumin-dextrose-catalase (ADC, Becton-Dickinson) or on Middlebrook 7H11 medium (Becton-Dickinson) supplemented with oleic acid-albumin-dextrose-catalase (OADC). When required, the media were added with 2% sucrose or the following concentrations of antibiotics: 20 µg ml⁻¹ of kanamycin and/or 50 µg ml⁻¹ of hygromycin and 25 µg ml⁻¹ of gentamicin.

Construction of KO mutant and complemented strains

Knockout mutants were constructed by allelic exchange using the Ts/*sacB* method (Pelicic *et al.*, 1997). Fragments bearing the genes of interest, 1000–1500 bp of flanking regions, and the *aph* gene were synthesized by PCR (see Table S1 for primer sequences). Amplicons corresponding to 5′ or 3′ flanking regions and kanamycin resistance cassette were digested with the appropriate restriction endonuclease (Table S2) and fragments obtained were cloned into BamHI-NotI or SpeI-NotI digested pPR27 vector. The resulting constructs were electroporated into *M. tuberculosis* for allelic replacement experiments. To obtain complemented strains, the cosmid I104 was used. The cosmid was electroporated into mutant strains and transformants were selected on Middlebrook 7H11 medium supplemented with 50 µg ml⁻¹ hygromycin. Resistant colonies were analysed for the pres-

ence of the integrated ESX-5 locus by PCR and/or Southern blot on genomic DNA.

RNA extraction and RT-PCR reactions

RNA was extracted from bacteria in exponential growth phase as previously described (Bottai *et al.*, 2011) and used in RT-PCR reactions using the SS-One Step RT-PCR kit (Invitrogen) in accordance with the manufacturer's instructions. Sequences of primers used are listed in Table S1.

Recombinant EsxN purification and production of EsxN antisera

The *esxN* coding sequence was amplified by PCR from H37Rv genomic DNA (see Table S1 for primer details) and cloned into pET303/CT-His vector (Invitrogen). Recombinant C-terminal 6His-tagged-EsxN (EsxN-6His) was expressed in *E. coli* BL21 (Invitrogen) and purified by affinity chromatography on Ni²⁺-NTA affinity columns (Invitrogen) under denaturing conditions. Briefly, binding of the protein to the column was performed in 20 mM sodium-phosphate buffer containing 6 M guanidine hydrochloride, 500 mM NaCl, pH 7.8. Elution of EsxN-6His was carried out in 20 mM sodium-phosphate buffer, 8 M urea, 500 mM NaCl, pH 4. Removal of contaminant proteins co-purified with EsxN-6His was obtained by electroelution of recombinant EsxN from polyacrylamide gel. To generate anti-EsxN polyclonal serum the protein preparation obtained was used for rabbit immunization using the mineral oil-based adjuvant Stimmune (Prionics) as recommended by the manufacturer.

Preparation of culture filtrates and total lysates from M. tuberculosis *strains and immunoblotting*

Preparation of mycobacterial culture filtrates was performed as previously described (Fortune *et al.*, 2005; Abdallah *et al.*, 2009). For analysis of EsxN secretion, *M. tuberculosis* strains were grown for 6 days in Sauton medium supplemented with 0.05% Tween 80. Mid-log phase bacteria were then resuspended in fresh Sauton medium and cultured for 4 days: cultures were harvested by centrifugation and culture filtrates were recovered after filtration through 0.22-µm-pore-size filters (Millipore MillexR GP), followed by concentration using Centricon filters with a 3 kDa cut-off (Millipore). Alternatively, following experimental protocols described elsewhere (Abdallah *et al.*, 2006; 2009), mycobacterial strains were grown to mid- or late logarithmic growth phase in Middlebrook 7H9 medium supplemented with 0.05% Tween 80. Precultures were then diluted in fresh Middlebrook 7H9 medium supplemented with 0.1% ADC. After 6 days, culture supernatants were recovered and proteins were precipitated with 10% TCA. To obtain total lysates, mycobacterial pellets were washed twice and resuspended in 20 mM Tris buffer (pH 7.5) and cells were broken by shaking with 106 µm acid washed-glass beads (Sigma-Aldrich) for 8 min in a Tissue Lyser apparatus (Qiagen). The supernatant fraction recovered after centrifugation at 5000 r.p.m. for 30 min represented the whole-cell lysate. Cell wall, cytosolic and membrane fractions

were prepared from total lysates by 60 min centrifugation at 14 000 r.p.m. (CW), followed by ultracentrifugation at 55 000 r.p.m. for 120 min (CYT and ME). Total protein concentration of samples obtained from mycobacterial cultures in Sauton medium was determined by using a Bradford protein assay (Sigma-Aldrich).

Immunoblot analyses were carried out with rabbit anti-PPE41 polyclonal serum (Abdallah *et al.*, 2006), rabbit anti-EsxN, a mouse monoclonal antibody raised against the PGRS domain of PE_PGRS33 (Abdallah *et al.*, 2009) or anti-EsxA (Hyb76-8, Antibodyshop, Statens Serum Institut). As control, culture supernatants were also analysed by Western blot for the presence of GroEL2 (anti-GroEL2 monoclonal antibody, Colorado State University, NIH, NIAID contract NO AI75320), and PPE68, a PPE protein encoded by the ESX-1 locus, reported to be associated to the mycobacterial cell envelope (Demangel *et al.*, 2004).

Two dimensional gel electrophoresis

Culture filtrates from *M. tuberculosis* strains grown in Sauton medium were concentrated in presence of EDTA-free protease inhibitor (Roche). Proteins were desalted and concentrated using the 2-D-Clean Up kit (GE Healthcare) and resuspended in 2D buffer (7 M urea, 4% CHAPS, 5 mM DTT, 2% ampholytes pH 4-6). Forty micrograms of protein was subjected to 2D gel electrophoresis using pH 4.5–5.5 immobilized gradient strips for the first dimension (15 min at 200 V, 20 min at 450 V, 20 min at 750 V and 105 min at 2000 V), and 4–20% sodium dodecyl sulphate-polyacrylamide gel electrophoresis (SDS-PAGE) for separation in the second dimension (120 min at 200 V). EsxN detection was performed by immunoblotting as mentioned above.

Proteinase K sensitivity assay

Proteinase-K treatment was performed as previously reported (Cascioferro *et al.*, 2007). Briefly, mycobacterial strains were grown in Middlebrook 7H9 medium for 6 days. Cells were washed in TBS buffer (150 mM NaCl, 3 mM KCl, 20 mM Tris-HCl, pH 7.5) and resuspended in 1 ml of the same buffer. Each sample was divided in two identical aliquots, one of which was added to proteinase K (Sigma-Aldrich) 100 µg ml^{-1}. Treated and untreated samples were incubated for 30 min at room temperature. The reaction was stopped adding 1× complete EDTA-free protease inhibitor (Roche). Samples were washed once in TBS and resuspended in 1× loading buffer (Sucrose 10% w/v, SDS 2% w/v, Tris-HCl 1.36 mM, bromophenol blue 0.01% w/v, β-mercaptoethanol 1% v/v). Equal amount of treated and untreated samples were loaded on polyacrylamide gel and tested in Western blotting as mentioned above.

SDS and drug sensitivity tests

Mutant, WT and complemented strains were grown to mid-logarithmic phase in Middlebrook 7H9 medium supplemented with 0.05% Tween 80. For detergent resistance/survival assay, bacterial cultures were diluted at a final OD$_{600}$ of 0.1,

and SDS was added to a final concentration of 0.1%. After 6, 24 and 72 h of incubation, the number of viable bacteria was determined.

Drug sensitivity assays were performed as previously described (Jackson *et al.*, 1999). Bacterial suspensions were plated on Middlebrook 7H11 medium containing twofold serial dilutions of ampicillin (3.125–6400 µg ml^{-1}), norfloxacin (0.3125–40 µg ml^{-1}), ofloxacin (0.03–4 µg ml^{-1}), bacitracin (1.56–800 µg ml^{-1}), vancomycin (0.3125–40 µg ml^{-1}), rifampicin (0.0075–0.24 µg ml^{-1}), isoniazid (0.125–2 µg ml^{-1}), ethambutol (0.8–6.4 µg ml^{-1}). As control, bacterial suspensions were plated on Middlebrook 7H11 medium without antibiotics. The number of viable bacteria was determined after incubation of plates at 37°C for 3 weeks. For each drug tested, the MIC value was defined as the lowest concentration of antibiotic that reduced the bacterial viability by at least 99% on solid medium. Microplate-based nitrate reductase assay was performed on mycobacterial cultures in exponential growth phase, as previously reported (Kumar *et al.*, 2005).

Macrophage infection assays

Bone marrow-derived macrophages were obtained from 8-week-old C57BL/6 mice. Cells were seeded in a 96-well plate at a density of 4×10^4 cells per well and differentiated into macrophages by culturing them for 7 days in RPMI medium (Gibco) supplemented with 10% heat-inactivated fetal calf serum, 10% L-cell conditioned medium, and 2 mM L-glutamine. Macrophages were infected with bacterial suspensions of *M. tuberculosis* H37Rv WT, KO and complemented strains at an moi of 1:1 (bacteria : cell). At 4 h, or 1, 4 and 7 days after infection, infected cells were lysed by the addition of 0.1% Triton X-100 (Fluka) in PBS. The number of intracellular bacteria was determined by plating serial dilutions of cell lysates on solid medium.

Mouse infection studies

Six-week-old CB17/Ico SCID mice (Charles River) were infected intravenously with 1×10^6 cfu per mouse of various mycobacterial strains. Three weeks after infection mice were sacrificed, and spleens and lungs were homogenized using an MM300 apparatus (Qiagen) and 2.5-mm-diameter glass beads. Serial fivefold dilutions of organ homogenates were plated on solid medium, and the cfu were counted after 3–4 weeks of incubation at 37°C. All animal studies were approved by the Institut Pasteur Safety Committee (Protocol 11.245; experimentation authorization number 75-1469), in accordance with European and French guidelines (Directive 86/609/CEE and Decree 87–848 of 19 October 1987).

References

Abdallah, A.M., Verboom, T., Hannes, F., Safi, M., Strong, M., Eisemberg, D., *et al.* (2006) A specific secretion system mediates PPE41 transport in pathogenic mycobacteria. *Mol Microbiol* **62:** 667–679.

Abdallah, A.M., Savage, N.D., van Zon, M., Wilson, L., Vandenbroucke-Grauls, C.M., van der Wel, N.N., *et al.* (2008) The ESX-5 secretion system of *Mycobacterium marinum* modulates the macrophage response. *J Immunol* **181:** 7166–7175.

Abdallah, A.M., Verboom, T., Weerdenburg, E.M., Gey van Pittius, N.C., Mahasha, P.W., Jimenez, C., *et al.* (2009) PPE and PE_PGRS proteins of *Mycobacterium marinum* are transported via the type VII secretion system ESX-5. *Mol Microbiol* **73:** 329–340.

Alderson, M.R., Bement, T., Day, C.H., Zhu, L., Molesh, D., Skeiky, Y.A.W., *et al.* (2000) Expression cloning of an immunodominant family of *Mycobacterium tuberculosis* antigens using human CD4(+) T cells. *J Exp Med* **191:** 551–560.

Bange, F.C., Collins, F.M., and Jacobs, W.R. (1999) Survival of mice infected with *Mycobacterium smegmatis* containing large DNA fragments from *Mycobacterium tuberculosis*. *Tuber Lung Dis* **79:** 171–180.

Banu, S., Honore, N., Saint-Joanis, B., Philpott, D., Prevost, M.C., and Cole, S.T. (2002) Are the PE-PGRS proteins of *Mycobacterium tuberculosis* variable surface antigens? *Mol Microbiol* **44:** 9–19.

Barry, C.E. 3rd (2001) Interpreting cell wall 'virulence factors' of *Mycobacterium tuberculosis. Trends Microbiol* **9:** 237–241.

Bitter, W., Houben, E.N., Bottai, D., Brodin, P., Brown, E.J., Cox, J.S., *et al.* (2009) Systematic genetic nomenclature for type VII secretion systems. *PLoS Pathog* **5:** e1000507.

Bottai, D., and Brosch, R. (2009) Mycobacterial PE, PPE and ESX clusters: novel insights into the secretion of these most unusual protein families. *Mol Microbiol* **73:** 325–328.

Bottai, D., Majlessi, L., Simeone, R., Frigui, W., Laurent, C., Lenormand, P., *et al.* (2011) ESAT-6 secretion-independent impact of ESX-1 genes *espF* and *espG1* on virulence of *Mycobacterium tuberculosis. J Infect Dis* **203:** 1155–1164.

Brennan, M.J., Delogu, G., Chen, Y., Bardarov, S., Kriakov, J., Alavi, M., and Jacobs, W.R. (2001) Evidence that mycobacterial PE_PGRS proteins are cell surface constituents that influence interactions with other cells. *Infect Immun* **69:** 7326–7333.

Brennan, P.J., and Nikaido, H. (1995) The envelope of mycobacteria. *Annu Rev Biochem* **64:** 29–63.

Brodin, P., Rosenkrands, I., Andersen, P., Cole, S.T., and Brosch, R. (2004) ESAT-6 proteins: protective antigens and virulence factors? *Trends Microbiol* **12:** 500–508.

Brodin, P., Majlessi, L., Marsollier, L., de Jonge, M.I., Bottai, D., Demangel, C., *et al.* (2006) Dissection of ESAT-6 system 1 of *Mycobacterium tuberculosis* and impact on immunogenicity and virulence. *Infect Immun* **74:** 88–98.

Brodin, P., Poquet, Y., Levillain, F., Peguillet, I., Larrouy-Maumus, G., Gilleron, M., *et al.* (2010) High content phenotypic cell-based visual screen identifies *Mycobacterium tuberculosis* acyltrehalose-containing glycolipids involved in phagosome remodeling. *PLoS Pathog* **6:** e1001100.

Cascioferro, A., Delogu, G., Colone, M., Sali, M., Stringaro, A., Arancia, G., *et al.* (2007) PE is a functional domain responsible for protein translocation and localization on mycobacterial cell wall. *Mol Microbiol* **66:** 1536–1547.

Chaturvedi, R., Bansal, K., Narayana, Y., Kapoor, N., Sukumar, N., Togarsimalemath, S.K., *et al.* (2010) The multifunctional PE_PGRS11 protein from *Mycobacterium tuberculosis* plays a role in regulating resistance to oxidative stress. *J Biol Chem* **285:** 30389–30403.

Cole, S.T., Brosch, R., Parkhill, J., Garnier, T., Churcher, C., Harris, D., *et al.* (1998) Deciphering the biology of *Mycobacterium tuberculosis* from the complete genome sequence. *Nature* **393:** 537–544.

Daleke, M.H., Cascioferro, A., de Punder, K., Ummels, R., Abdallah, A.M., van der Wel, N.N., *et al.* (2011) Conserved Pro-Glu (PE) and Pro-Pro-Glu (PPE) protein domains target LipY lipases of pathogenic mycobacteria to the cell surface via the ESX-5 pathway. *J Biol Chem* **286:** 19024–19034.

Delogu, G., and Brennan, M.J. (2001) Comparative immune response to PE and PE_PGRS antigens of *Mycobacterium tuberculosis. Infect Immun* **69:** 5606–5611.

Demangel, C., Brodin, P., Cockle, P.J., Brosch, R., Majlessi, L., Leclerc, C., *et al.* (2004) Cell envelope protein PPE68 contributes to *Mycobacterium tuberculosis* RD1 immunogenicity independently of a 10-kilodalton culture filtrate protein and ESAT-6. *Infect Immun* **72:** 2170–2176.

Fortune, S.M., Jaeger, A., Sarracino, D.A., Chase, M.R., Sassetti, C.M., Sherman, D.R., *et al.* (2005) Mutually dependent secretion of proteins required for mycobacterial virulence. *Proc Natl Acad Sci USA* **102:** 10676–10681.

Frigui, W., Bottai, D., Majlessi, L., Monot, M., Josselin, E., Brodin, P., *et al.* (2008) Control of *M. tuberculosis* ESAT-6 secretion and specific T cell recognition by PhoP. *PLoS Pathog* **4:** e33.

Gao, L.Y., Pak, M., Kish, R., Kajihara, K., and Brown, E.J. (2006) A mycobacterial operon essential for virulence in vivo and invasion and intracellular persistence in macrophages. *Infect Immun* **74:** 1757–1767.

Garces, A., Atmakuri, K., Chase, M.R., Woodworth, J.S., Krastins, B., Rothchild, A.C., *et al.* (2010) EspA acts as a critical mediator of ESX1-dependent virulence in *Mycobacterium tuberculosis* by affecting bacterial cell wall integrity. *PLoS Pathog* **6:** e1000957.

Gey van Pittius, N.C., Gamieldien, J., Hide, W., Brown, G.D., Siezen, R.J., and Beyers, A.D. (2001) The ESAT-6 gene cluster of *Mycobacterium tuberculosis* and other high G+C Gram-positive bacteria. *Genome Biol* **2:** RESEARCH0044.

Gey van Pittius, N.C., Sampson, S.L., Lee, H., Kim, Y., van Helden, P.D., and Warren, R.M. (2006) Evolution and expansion of the *Mycobacterium tuberculosis* PE and PPE multigene families and their association with the duplication of the ESAT-6 (*esx*) gene cluster regions. *BMC Evol Biol* **6:** 95.

Gordon, S.V., Bottai, D., Simeone, R., Stinear, T.P., and Brosch, R. (2009) Pathogenicity in the tubercle bacillus: molecular and evolutionary determinants. *Bioessays* **31:** 378–388.

Griffin, J.E., Gawronski, J.D., Dejesus, M.A., Ioerger, T.R., Akerley, B.J., and Sassetti, C.M. (2011) High-resolution phenotypic profiling defines genes essential for mycobac-

terial growth and cholesterol catabolism. *PLoS Pathog* **7:** e1002251.

Jackson, M., Raynaud, C., Laneelle, M.A., Guilhot, C., Laurent-Winter, C., Ensergueix, D., *et al.* (1999) Inactivation of the antigen 85C gene profoundly affects the mycolate content and alters the permeability of the *Mycobacterium tuberculosis* cell envelope. *Mol Microbiol* **31:** 1573–1587.

Jain, S.K., Hernandez-Abanto, S.M., Cheng, Q.J., Singh, P., Ly, L.H., Klinkenberg, L.G., *et al.* (2007) Accelerated detection of *Mycobacterium tuberculosis* genes essential for bacterial survival in guinea pigs, compared with mice. *J Infect Dis* **195:** 1634–1642.

Jones, G.J., Gordon, S.V., Hewinson, R.G., and Vordermeier, H.M. (2010) Screening of predicted secreted antigens from *Mycobacterium bovis* reveals the immunodominance of the ESAT-6 protein family. *Infect Immun* **78:** 1326–1332.

Karboul, A., Mazza, A., Gey van Pittius, N.C., Ho, J.L., Brousseau, R., and Mardassi, H. (2008) Frequent homologous recombination events in *Mycobacterium tuberculosis* PE/PPE multigene families: potential role in antigenic variability. *J Bacteriol* **190:** 7838–7846.

Kumar, M., Khan, I.A., Verma, V., Kalyan, N., and Qazi, G.N. (2005) Rapid, inexpensive MIC determination of *Mycobacterium tuberculosis* isolates by using microplate nitrate reductase assay. *Diagn Microbiol Infect Dis* **53:** 121–124.

Li, Y., Miltner, E., Wu, M., Petrofsky, M., and Bermudez, L.E. (2005) A *Mycobacterium avium* PPE gene is associated with the ability of the bacterium to grow in macrophages and virulence in mice. *Cell Microbiol* **7:** 539–548.

MacGurn, J.A., Raghavan, S., Stanley, S.A., and Cox, J.S. (2005) A non-RD1 gene cluster is required for Snm secretion in *Mycobacterium tuberculosis*. *Mol Microbiol* **57:** 1653–1663.

McLaughlin, B., Chon, J.S., MacGurn, J.A., Carlsson, F., Cheng, T.L., Cox, J.S., and Brown, E.J. (2007) A mycobacterium ESX-1-secreted virulence factor with unique requirements for export. *PLoS Pathog* **3:** e105.

Pallen, M. (2002) The ESAT-6/WXG100 superfamily – and a new Gram-positive secretion system? *Trends Microbiol* **10:** 209–212.

Pandey, A.K., and Sassetti, C.M. (2008) Mycobacterial persistence requires the utilization of host cholesterol. *Proc Natl Acad Sci USA* **105:** 4376–4380.

Pelicic, V., Jackson, M., Reyrat, J.M., Jacobs, W.R., Gicquel, B., and Guilhot, C. (1997) Efficient allelic exchange and transposon mutagenesis in *Mycobacterium tuberculosis*. *Proc Natl Acad Sci USA* **94:** 10955–10960.

Pym, A.S., Brodin, P., Majlessi, L., Brosch, R., Demangel, C., Williams, A., *et al.* (2003) Recombinant BCG exporting ESAT-6 confers enhanced protection against tuberculosis. *Nat Med* **9:** 533–539.

Ramakrishnan, L., Federspiel, N.A., and Falkow, S. (2000) Granuloma-specific expression of mycobacterium virulence proteins from the glycine-rich PE-PGRS family. *Science* **288:** 1436–1439.

Ren, H., Dover, L.G., Islam, S.T., Alexander, D.C., Chen, J.M., Besra, G.S., and Liu, J. (2007) Identification of the lipooligosaccharide biosynthetic gene cluster from *Mycobacterium marinum*. *Mol Microbiol* **63:** 1345–1359.

Sampson, S.L., Lukey, P., Warren, R.M., van Helden, P.D., Richardson, M., and Everett, M.J. (2001) Expression, characterization and subcellular localization of the *Mycobacterium tuberculosis* PPE gene Rv1917c. *Tuberculosis (Edinb)* **81:** 305–317.

Sani, M., Houben, E.N., Geurtsen, J., Pierson, J., de Punder, K., van Zon, M., *et al.* (2010) Direct visualization by cryo-EM of the mycobacterial capsular layer: a labile structure containing ESX-1-secreted proteins. *PLoS Pathog* **6:** e1000794.

Simeone, R., Bottai, D., and Brosch, R. (2009) ESX/type VII secretion systems and their role in host-pathogen interaction. *Curr Opin Microbiol* **12:** 4–10.

Song, H., Sandie, R., Wang, Y., Andrade-Navarro, M.A., and Niederweis, M. (2008) Identification of outer membrane proteins of *Mycobacterium tuberculosis*. *Tuberculosis (Edinb)* **88:** 526–544.

Stinear, T.P., Seemann, T., Harrison, P.F., Jenkin, G.A., Davies, J.K., Johnson, P.D., *et al.* (2008) Insights from the complete genome sequence of *Mycobacterium marinum* on the evolution of *Mycobacterium tuberculosis*. *Genome Res* **18:** 729–741.

Tekaia, F., Gordon, S.V., Garnier, T., Brosch, R., Barrell, B.G., and Cole, S.T. (1999) Analysis of the proteome of *Mycobacterium tuberculosis in silico*. *Tuber Lung Dis* **79:** 329–342.

Uplekar, S., Heym, B., Friocourt, V., Rougemont, J., and Cole, S.T. (2011) Comparative genomics of *esx* genes from clinical isolates of *Mycobacterium tuberculosis* provides evidence for gene conversion and epitope variation. *Infect Immun* **79:** 4042–4049.

Voskuil, M.I., Schnappinger, D., Rutherford, R., Liu, Y., and Schoolnik, G.K. (2004) Regulation of the *Mycobacterium tuberculosis* PE/PPE genes. *Tuberculosis (Edinb)* **84:** 256–262.

Weerdenburg, E.M., Abdallah, A.M., Mitra, S., de Punder, K., van der Wel, N.N., Bird, S., *et al.* (2012) ESX-5-deficient *Mycobacterium marinum* is hypervirulent in adult zebrafish. *Cell Microbiol* doi: 10.1111/j.1462-5822.2012.01755.x [Epub ahead of print].

Supporting information

Additional supporting information may be found in the online version of this article.

Please note: Wiley-Blackwell are not responsible for the content or functionality of any supporting materials supplied by the authors. Any queries (other than missing material) should be directed to the corresponding author for the article.